Energy Storage Materials 6 (2017) 18–25

Contents lists available at ScienceDirect

Energy Storage Materials

journal homepage: www.elsevier.com/locate/ensm

The gap between long lifespan Li-S coin and pouch cells: The importance of lithium metal anode protection

Xin-Bing Cheng [a,1], Chong Yan [a,b,1], Jia-Qi Huang [a,d], Peng Li [a,c], Lin Zhu [a,e,c], Lida Zhao [a,c], Yingying Zhang [a,c], Wancheng Zhu [e], Shu-Ting Yang [b], Qiang Zhang [a,*]

[a] Beijing Key Laboratory of Green Chemical Reaction Engineering and Technology, Department of Chemical Engineering, Tsinghua University, Beijing 100084, PR China
[b] National & Local Joint Engineering Laboratory for Motive Power and Key Materials, College of Chemistry and Chemical Engineering, Henan Normal University, Xinxiang 453007, PR China
[c] North Guoneng Technology, Beijing Tsingna Technology Co., Ltd., Beijing 100084, PR China
[d] Advanced Research Institute for Multidisciplinary Science, Beijing Institute of Technology, Beijing 100081, PR China
[e] Department of Chemical Engineering, Qufu Normal University, Shandong 273165, PR China

ARTICLE INFO

Article history:
Received 30 August 2016
Received in revised form
13 September 2016
Accepted 13 September 2016

Keywords:
Li-S battery
Pouch cell
Polysulfides
Li metal anode
Electrolyte

ABSTRACT

Lithium-sulfur (Li-S) batteries have been strongly regarded as next-generation energy storage devices for their very high theoretical energy density (2600 W h kg^{-1}), low cost, and non-toxicity. Li polysulfide (LiPS) shuttle in the cathode and Li dendrite growth in the anode are among the toughest issues on the practical applications of Li-S batteries. By efficient cathode and membrane design, LiPS can be effectively trapped in the cathode side and the coin cells deliver a superior cycling performance of 2000 cycles. When the coin cell strategy is transplanted to a pouch cell, the possibility to achieve a long-lifespan Li-S pouch cell should be further explored. Herein, the gaps between the coin and pouch cell were probed and the failure mechanism of a Li-S pouch cell was explored. Compared with LiPS shuttle issue, Li metal powdering and the induced polarization are more responsible for pouch cell failure. Electrochemical cycling performance and *ex-situ* morphology characterization indicated that the continuously striping/plating of Li ions results in Li dendrite growth during cycling test, which exposes more fresh Li to electrolyte and induces the formation of dead Li powder. Therefore, the Li ion diffusion resistance is increased and the Coulombic efficiency is reduced gradually. When the cycled Li anode was updated by a fresh Li metal, the renaissance cell with cycled cathode *vs* fresh anode exhibited an improved discharge capacity from 314 to 1030 mA h g^{-1} at 0.1 C. Relatively to a neglected role in coin cells in most cases, Li metal anode tremendously affects long-term cycling performance of Li-S pouch cells. More attentions should be concentrated on efficiently protecting Li metal anode to achieve large capacity and safe Li-S cells with high energy density.

1. Introduction

Due to the accelerating potential of electrochemical energy storage and popularity of mobile life [1], next-generation batteries with high capacity, high energy/power density, and low cost are strongly considered [2,3]. When viewing the periodic table of elements, it's easy to confirm the metallic lithium (Li) has the most negative potential (−3.040 V *vs* the standard hydrogen electrode) and highest specific capacity (3861 mA h g^{-1}) [4,5]. This renders Li metal among the best candidates for rechargeable battery anode [1,4,6]. Among various cathode materials, sulfur (S) has a theoretical capacity of 1675 mA h g^{-1} with the abundant and environmentally benign nature, which is a superior candidate for cathode material [7]. Consequently, Li-S battery has been highly investigated as the next-generation battery energy storage systems with a theoretical gravimetric energy densities of 2600 W h kg^{-1}. Increasing attention is paid on Li-S batteries to address impending energy and environmental issues [8,9], as well as explode novel energy storage system for future portable and wearable devices [10,11].

The multi-electron transfer chemistry based on Li and S couple contributes to high energy density of a Li-S cell [2,12]. However, the formation of soluble Li polysulfides (LiPSs) induces a very complex couple between the redox and diffusion of LiPSs in a working cell. Some LiPSs are attached onto separators and other

* Corresponding author.
E-mail address: zhang-qiang@mails.tsinghua.edu.cn (Q. Zhang).
[1] These authors contributed equally to this work.

http://dx.doi.org/10.1016/j.ensm.2016.09.003
2405-8297/

dead space in a cell, which are corresponding loss of active materials and therefore capacity decay of Li-S cell [10,13]. Beyond that, Li dendrite growth on the anode surface also induces notorious short circuit and safety issue [14,15].

With the rapid progress in the field of materials chemistry and nanotechnology, Li-S batteries have been extensively explored. For instance, efficient cathode designs based on LiPS confinement through physical barrier [16–19] and chemical anchoring [20–25], as well as the permselective separator/interlayer [26–30] have been are proposed to minimize the shuttle of LiPSs and reach high sulfur utilization. The uncontrolled dendrite growth gives rise to poor safety assurance, low utilization of Li metal anode, and inevitably deteriorating the performance of Li-S cells. Recently, Li metal dendrites can be effectively inhibited by employing solid/polymer electrolyte [31,32], stable and optimized solid electrolyte interphase (SEI) [6,15,33–35], and rational design of structured anode [36,37]. The introduction of multifunctional separators and modified electrolyte in a Li-S cell also significantly contribute to the long-term cycling stability [10,27,38]. Up to now, Li-S batteries based on coin cells have achieved a superior cycling stability, including very high S loading (3–20 mg cm^{-2}) [39,40], ultra-long cycling period (500–2000 cycles) [41,42], and superb capacity retention (50–80%) [43]. However, relative to the shining performance based on coin cells, few pouch cells have been declared in scientific publication.

The evaluation of energy materials in a pouch cell is a necessary step to probe the stability of electrode and Li storage performance towards practical cells for further applications in unmanned vehicles, satellites, electrical vehicles and portable devices working at harsh conditions. Compared to coin cells, the large areal loading of sulfur as active materials in pouch cells not only leads to severer LiPS shuttle, but also large areal current on the Li anode. Let's take 1500 mA h pouch cell as a typical example (average capacity for a smartphone). If the cell is discharged at 0.1 C (1.0 C = 1675 mA g^{-1}, assuming the capacity is 1000 mA h g^{-1}), the applied current to the anode is estimated as 160 mA, which is much larger than these on a coin cell (0.5–5 mA). The large areal current cannot uniformly distribute on the anode surface and may result in Li dendrite growth in most cases [44]. Therefore, there are huge gaps between the coin cells and pouch cells based on multi-electron conversion chemistry based on Li and S couples.

In this contribution, the failure mechanism of a 1500 mA h Li-S pouch cell (Fig. 1a) was investigated by electrochemical cycling performance, electrochemical impedance spectroscopy (EIS), and morphology evolution characterization. For a coin cell with a thick Li metal and small current density, capacity decay of a Li-S cell mainly suffers from the shuttle of LiPSs. However, the situation is greatly different for a Li-S pouch cell with high sulfur loading. We found Li metal powdering and the induced polarization took most responsibility for discharge capacity loss in a working pouch cell (Fig. 1b). The continuous plating/striping of Li ion results in Li dendrite growth during cycling and corrodes Li metal into irreversible dead and powdering Li. These severely increase Li ion diffusion resistance and reduces Coulombic efficiency. Relative to the superior cycling performance of Li-S coin cells, the electrochemical performance of Li-S pouch cells should be further enhanced.

2. Results and discussion

2.1. Electrochemical long-term cycling performance

To probe the evolution of electrode in a working cell, we fabricated pouch cells through a layer-by-layer strategy with five pieces of cathode and four pieces of anode as a group. The total cell was composed of three groups. The area of each electrode was 15 cm^2 (50 mm × 30 mm). A high areal sulfur loading of 4.43 mg cm^{-2} and a total sulfur content of 1596.6 mg was achieved in the pouch cell.

The pouch cell reached an initial discharge capacity of 1920 mA h (1207 mA h g^{-1}) at 0.1 C (1.0 C = 1675 mA g^{-1}) (Fig. 2a). The high capacity was followed by a rapid decrease, which is attributed from the irreversible dissolution of high order polysulfides into the electrolyte and the formation of solid electrolyte interfaces (SEI) on the Li metal anode [13]. A stable capacity of 1350 mA h (846 mA h g^{-1}) was achieved before 60th cycle. However, the pouch cell got another rapid capacity and Coulombic efficiency decay at 60th cycle. A discharge capacity of 500 mA h (314 mA h g^{-1}) was preserved at 100th cycle.

In order to probe the reason of pouch cell failure, the charge/discharge profiles were investigated (Fig. 2b). A two-stage discharge route was exhibited, which were corresponding reductions of sulfur into LiPSs and LiPSs to lithium sulfides at *ca.* 2.31 and 2.10 V, respectively. The rapid capacity decay at the initial 5 cycles was mainly ascribed to the capacity loss contributed by the precipitation of solid Li_2S_2/Li_2S from soluble LiPSs onto conductive framework. With the continuous cycling before 70th cycle, the voltages of both the high and low platforms kept an almost constant value, confirming the stable cycling of Li-S pouch cells. After that, a significant decay of discharge capacity and Coulombic efficiency was recorded at 70th cycle. The voltages of high and low voltage platforms decreased sharply from 2.31 to 2.19 V and 2.10 to 1.99 V, respectively, demonstrating a largely increased polarization. The increase in polarization during cycling test is responsible for the deteriorative cycling performance.

To quantitatively describe the sluggish kinetic of polysulfide redox in a cycled pouch cell, a detailed lower-platform voltage evolution in the whole lifespan of pouch cell was recorded. The lower platform voltage in discharge curves was defined as the voltage to approximatively bisect the capacity of the lower platform in the discharge curve (the insert of Fig. 2c). The lower platform voltage indicated a similar trend with discharge capacity. A rapid decay of lower-platform voltage is still observed at 70th cycle, indicating the rise of overpotential resulting from soluble LiPSs to solid Li_2S_2/Li_2S.

The long-term cycling test of the Li-S pouch cells clearly demonstrated that the large decay of discharge capacity and Coulombic efficiency was attributed to continuously increased polarization during cycling. Li dendrite growth in the anode as well as LiPS dissolution in the cathode can be responsible for the increased polarization [45]. To decouple the origin of large polarization in pouch cells, a control coin cell was assembled with the same sulfur loading of 4.43 mg cm^{-2}. Though with a small decay during 200 cycles at 0.5 C, the cell can work stably with a low-platform voltage of 2.05 V (Fig. S1). Compared with coin cells, pouch cells are with the same areal sulfur loading of 4.43 mg cm^{-2}, but an increased total S content from 11.76 to 1596.6 mg in the whole cell and an enhanced current of 9.85 to 159.66 mA on the anode surface. The increased current on the anode leads to large dendrite growth, which is the prime difference of Li-S pouch and coin cells. The dendrite growth in the anode side and thus-induced polarization renders a notorious cycling stability of Li-S pouch cells. We will further check the morphology/structure of anode and cathode to ascertain the evolution of electrode in a working cell and probe the failure mechanism of Li-S pouch cells.

2.2. Morphology evolution of electrode in a working pouch cell

A fresh Li metal anode is always with uneven surface, which can potentially be the nucleating cites for dendrite growth

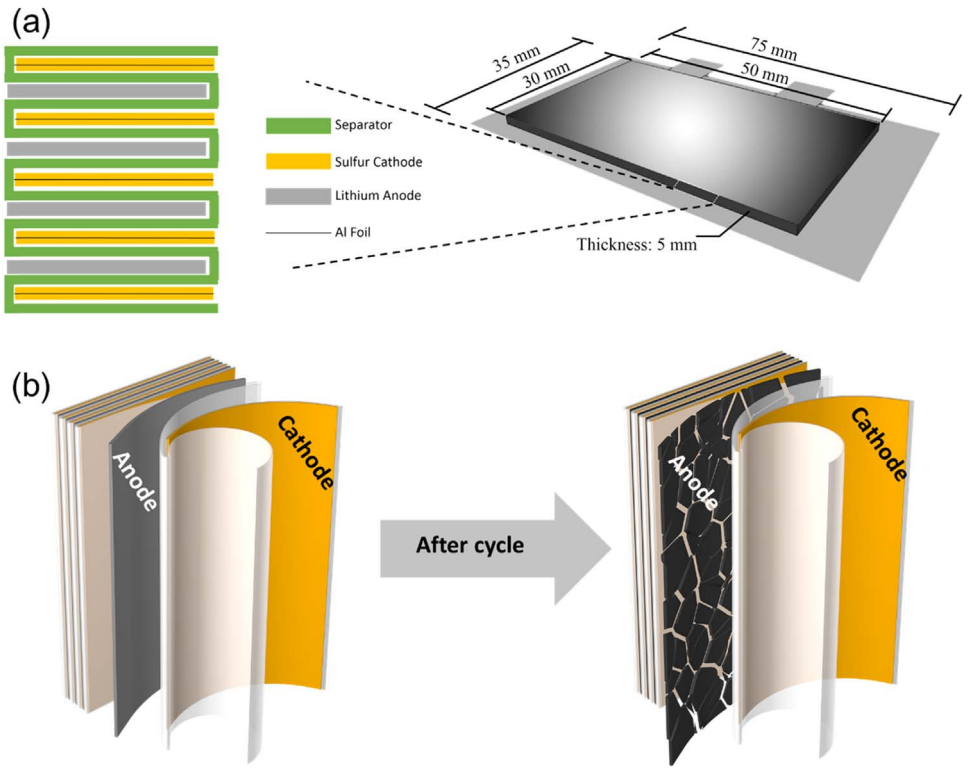

Fig. 1. Schematic illustration of Li-S pouch cells. (a) Schematic diagram of internal structure of a pouch cell and its size parameters. (b) Li metal anode evolution during cycles.

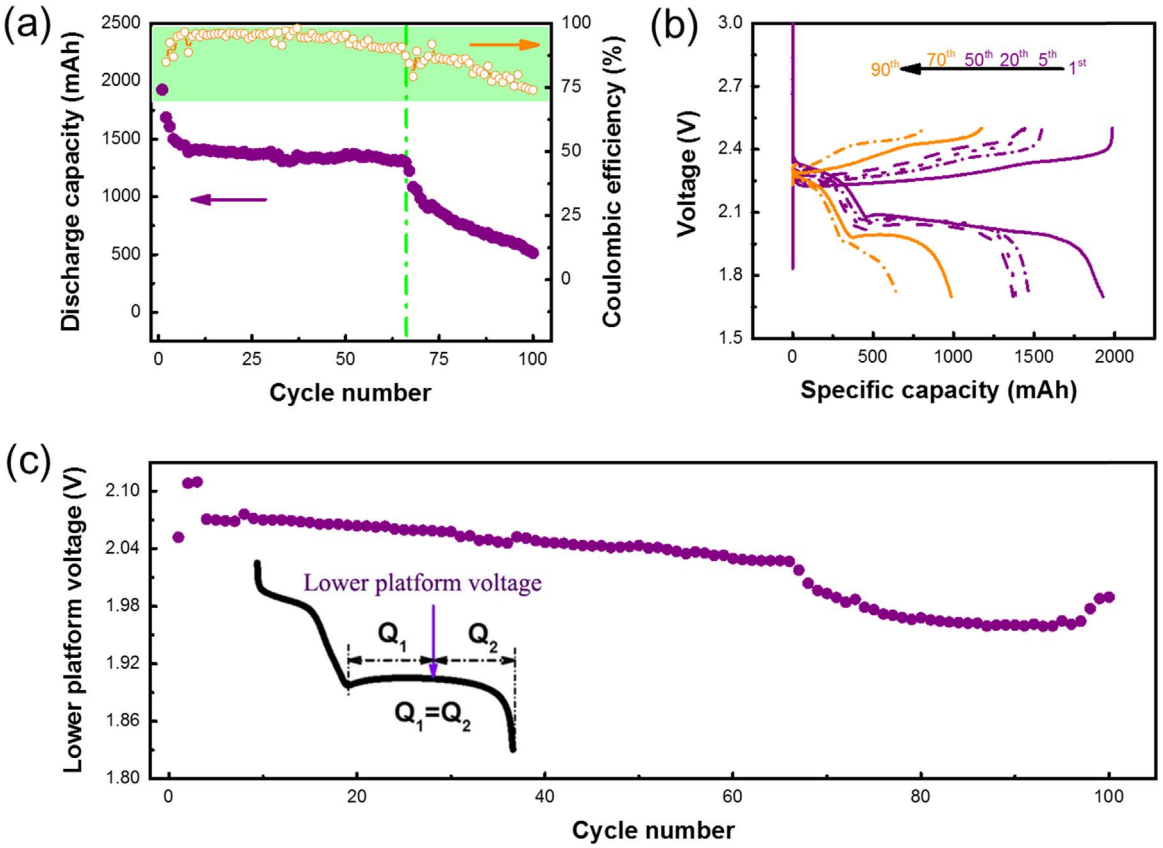

Fig. 2. Electrochemical cycling performance of Li-S pouch cells. (a) Discharge capacity and Coulombic efficiency of the pouch cell at a current density of 167.5 mA g^{-1} (0.1 C). (b) Galvanostatic discharge/charge curves of Li-S pouch cell at different cycles. (c) Evolution of lower platform voltage during cycling test. The inset figure is the definition of lower platform voltage.

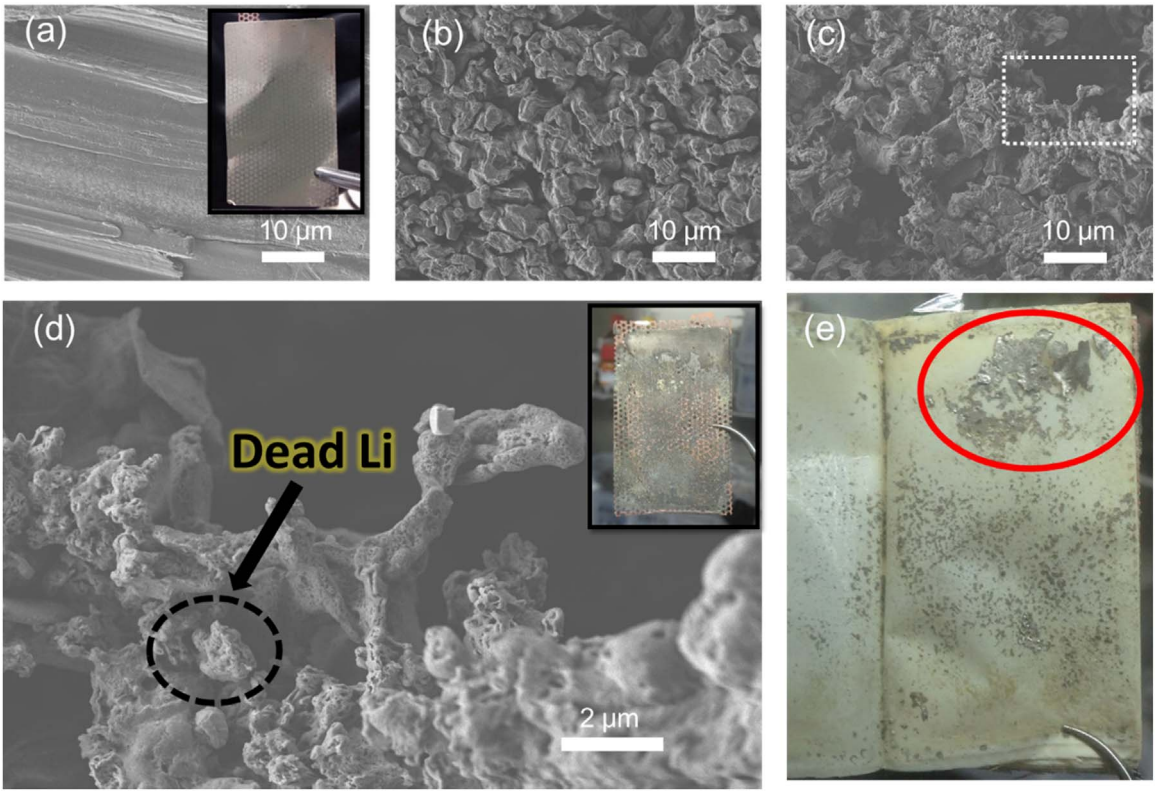

Fig. 3. Morphology evolution of Li metal anode during cycling test of Li-S pouch cells. SEM images of Li anode (a) before cycles, after (b) 20 cycles and (c) 100 cycles in the pouch cell. (d) The locally enlarged SEM image of the square area in (c). The inset picture in (d) is the optical morphology of cycled Li metal electrode in a pouch cell. (e) Optical images of dead and powdery Li on the separator.

(Fig. 3a). As Li dendrite growth is strongly affected by the applied current density, it is difficult to observe Li dendrites on the anode surface due to the small current (2 mA at 0.1 C on coin cell) (Fig. S2). However, the current applied in a pouch cell was increased by a range of several dozen to hundred times (160 mA at 0.1 C), resulting in the facile Li dendrite nucleation and continuous growth. The anode surface was largely covered by Li dendrites after 20 cycles in a pouch cell (Fig. 3b). The pristine dense surface was replaced by a porous and powdery Li metal, leading to an enhanced contact area and reactions between Li metal and organic electrolyte. The fresh Li metal consumed liquid electrolyte to form SEI. If the powdery Li with SEI wrapping got away from the current collector, dead Li particles are achieved.

With the continuous plating/stripping on the anode after 100 cycles, Li powdering issues became more severe (Fig. 3c and d). The optical morphology of Li electrode after 100th cycling was totally different from that of the initial electrode. Powdery Li distributed in homogeneously on the current collector (the inset in Fig. 3d). More powdery Li broke away from the conductive matrix to form dead Li, resulting in reduced Coulombic efficiency and increased polarization. Due to the weak combination of deposited Li and current collector, large amounts of dead Li were found on the polypropylene separator (Fig. 3e). When the disassembled pouch cell was taken out of glove box and exposed to air, powdery Li self-ignited because of the largely increased contact area between Li metal and air (Fig. S3a and b). Relative to dramatic changes of anode morphology in a pouch cell, the morphology of sulfur cathode was preserved well (Fig. S3c and d). Consequently, powdering and dead Li in a working Li-S pouch cell took a prime responsibility for long-term cycling instability, which is very consistent with the previous electrochemical tests [35,45]. The effective anode protection in a working Li-S batteries is a necessary step to achieve a practical cell [46–49].

2.3. Electrochemical cycling performance of renaissance cell

To further investigate the failure mechanism of Li-S pouch cells, three renaissance cells were assembled based on failure cells: new pouch cell by employing fresh electrolyte into cycled pouch cell (Fig. 4a), coin cells with cycled cathode *vs* fresh anode (Fig. 4b), and fresh cathode *vs* cycled anode (Fig. 4c).

Li powdering largely increased the surface area of Li metal anode and thus severe reactions between Li metal and electrolyte, which can dry the cells after long-term cycling. When fresh electrolyte was injected to the failed pouch cell, the discharge capacity can be increased from 500 to 900 mA h (566 mA h g^{-1}) (Fig. 4a). However, fresh electrolyte still can not preserve the high capacity and this renaissance pouch cell got rapid capacity decay. Therefore, except the consumption of electrolyte in a cell, both cathode and anode should be also checked to distinguish their roles on the capacity decay.

Based on this consideration, another two renaissance cells with fresh anode and cathode were assembled with cycled cathode and anode. The cycled pouch cell was disassembled at the end of 100th charging. The obtained Li anode and sulfur cathode were sufficiently washed using DME solvent to remove lithium salts and partial soluble LiPS species. After drying, Li-S coin cells were assembled with the cycled cathode *vs* fresh anode and fresh cathode *vs* cycled anode.

The renaissance cell with cycled cathode *vs* fresh anode indicated an improved discharge capacity from 314 to 1030 mA h g^{-1} (Fig. 4b) at 0.1 C and remained stable in the following cycles (999 mA h g^{-1} at 15th cycle) with a high Coulombic efficiencies (78.13% at 15th cycle). However, the renaissance cell with fresh cathode *vs* cycled anode just achieved a capacity of 495 mA h g^{-1} at 0.1 C, which was a very small increase compared with the cycled pouch cell (314 mA h g^{-1}). Though with a little

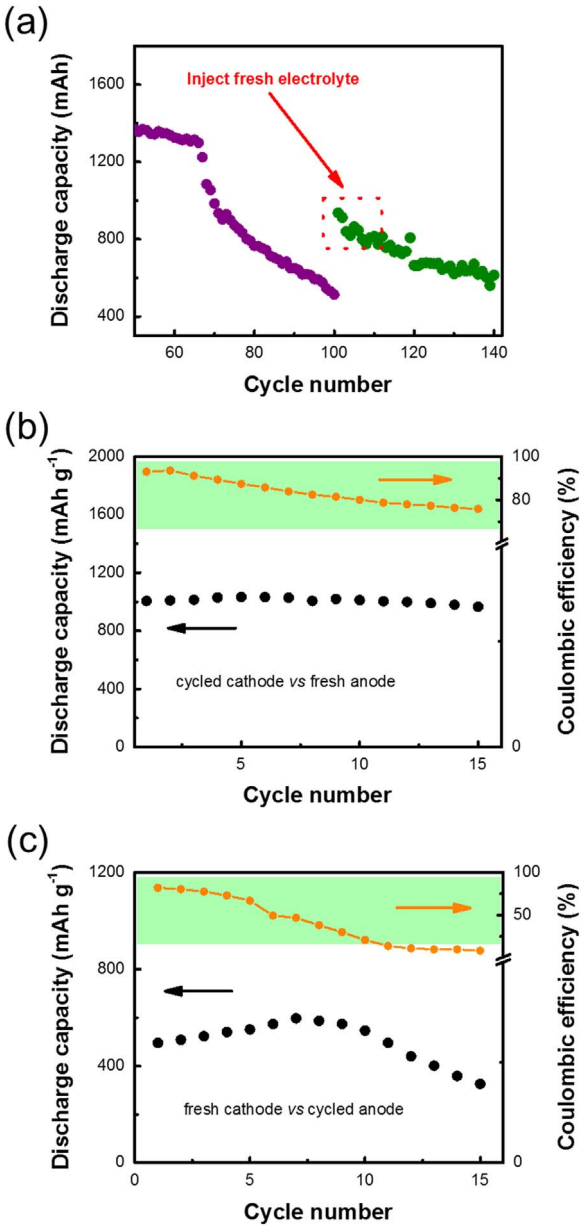

Fig. 4. Electrochemical cycling performance of renaissance Li-S cells. (a) Cycling performance after re-injecting organic electrolyte into a pouch cell at 0.75 mA cm^{-2}. Cycling performance of the reassembled coin cell with (b) cycled cathode *vs* fresh anode and (c) fresh cathode *vs* cycled anode.

increase at 8th cycle, the discharge capacity decayed to 358 mA h g^{-1} with a low Coulombic efficiency of 10.04% at 15th cycle (Fig. 4c). Relative to an updated sulfur cathode, it clearly indicated an updated anode can greatly improve the cycling performance of cycled pouch cell with high sulfur loading. Consequently, anode issue induced by Li powdering and dead Li at large current density contributed to the capacity degradation and poor cycling stability of a Li-S pouch cell.

2.4. The evolution of resistance in a pouch cell

To probe the internal Li ion diffusion, electrochemical impedance spectroscopy (EIS) at different cycles were collected. After the activation at 1st cycle, the impedance of pouch cell was increasing with continuous cycles (Fig. 5a). A classic model was employed to interpret EIS spectrum and R_{ct} was employed to represent Li ion diffusion in the anode matrix (Supplementary Text 1). R_{ct} was increasing during cycles from 0.140 Ω after 1st cycle to 2.112 Ω after 100th cycle (Fig. 5b). Therefore, Li ion diffusion in the anode matrix and whole cell was severely hindered.

Li ion diffusion behavior in a pouch cell was further quantified by Li ion diffusion coefficient (D_{Li^+}) and exchange current density (j_0) (Supplementary Text 2) [50]. D_{Li^+} and j_0 indicated a similar decreasing trend from 2.51×10^{-14} to 1.50×10^{-18} cm^{-2} S^{-1} and 4.40×10^{-4} to 3.38×10^{-5} A cm^{-2}, respectively. These results demonstrated that the charge transfer speed became slower and reversible electrochemical reaction got worse during cycling. The continuously reduced D_{Li^+} and j_0 confirmed large polarization and Li ion diffusion resistance induced by powdering and dead Li in the pouch cells.

2.5. Proposed failure mechanism

Coin cells are mostly accepted for material performance evaluation in most researches. Li metal anode are much overloaded. Consequently, the performance of cathode materials and separator can be fully demonstrated. To probe the potential use of sulfur and lithium for practical cells, pouch cells with high sulfur loadings are employed. However, the cycling life of pouch cells is shorter than the one assembled as a coin cell.

When the coin and pouch cells are operated at the same areal current density, the total current in a pouch cell is much larger than that of a coin cell. On one hand, the amounts of as-obtained LiPSs in the pouch cells are much larger than those in coin cells; therefore, the shuttle of polysulfides became severe [45]. On the other hand, the current density applied onto Li metal anode was much enhanced, which induced a large concentration gradient of Li ions at a high current rate. The SEI layer attached on Li metal anode is not stable with high concentration of LiPSs and large fluctuation of Li ions [35]. Therefore, compared to the functional role of $LiNO_3$ in coin cell [48], the SEI layer formed by $LiNO_3$ in the pouch cell prefers to break down due to the corrosion of high concentration of LiPS and mechanical destruction of Li dendrites. The damaged SEI layer in return aggravates Li dendrite growth. When the dendritic Li are detached from the Li foil, dead Li are obtained and Li active materials are loss. Powdery Li increases the contact area and reactions between Li metal and electrolyte. The largely consumed electrolyte results in the increase of viscosity and Li ion diffusion resistance. Therefore, the polarization of pouch cell increased gradually. The continuous consumption of organic electrolyte induces the dry cell. Once the electrolyte can't penetrate through the 3D electrode, a rapid capacity loss after stable cycling was observed in a pouch cell. It should be noted that the damage induced by powdery Li is irreversible and re-injecting electrolyte also cannot save pouch cell due to the fatal failure of Li metal matrix. Therefore, the robust use of Li metal anode is a great challenge for a pouch cell with high cycling life. More attention should be concentrated on Li metal anode protection.

2.6. Possible strategies to protect Li metal in pouch cells

Due to the rising researches of Li-S and Li-oxygen batteries, great attention has been paid on Li metal anodes recently. Several strategies have been proposed to handle the Li dendrite induced safety concern and poor lifespan [4,51]. One of the most convenient methods is electrolyte modification. Cs cations [33], FEC [52], LiF [53], LiBOB [54], $LiNO_3$/LiPS hybrid [15,38], highly concentrated electrolyte [6,55] have indicated a large potential in suppressing Li dendrite growth. The other method is to design a highly efficient conductive matrix for Li plating/stripping. Due to the above discussions from the anode view, Li-S pouch cell is more possible to be failed by the high polarization caused by powdery dead Li. The conductive matrix can not only suppress Li dendrite

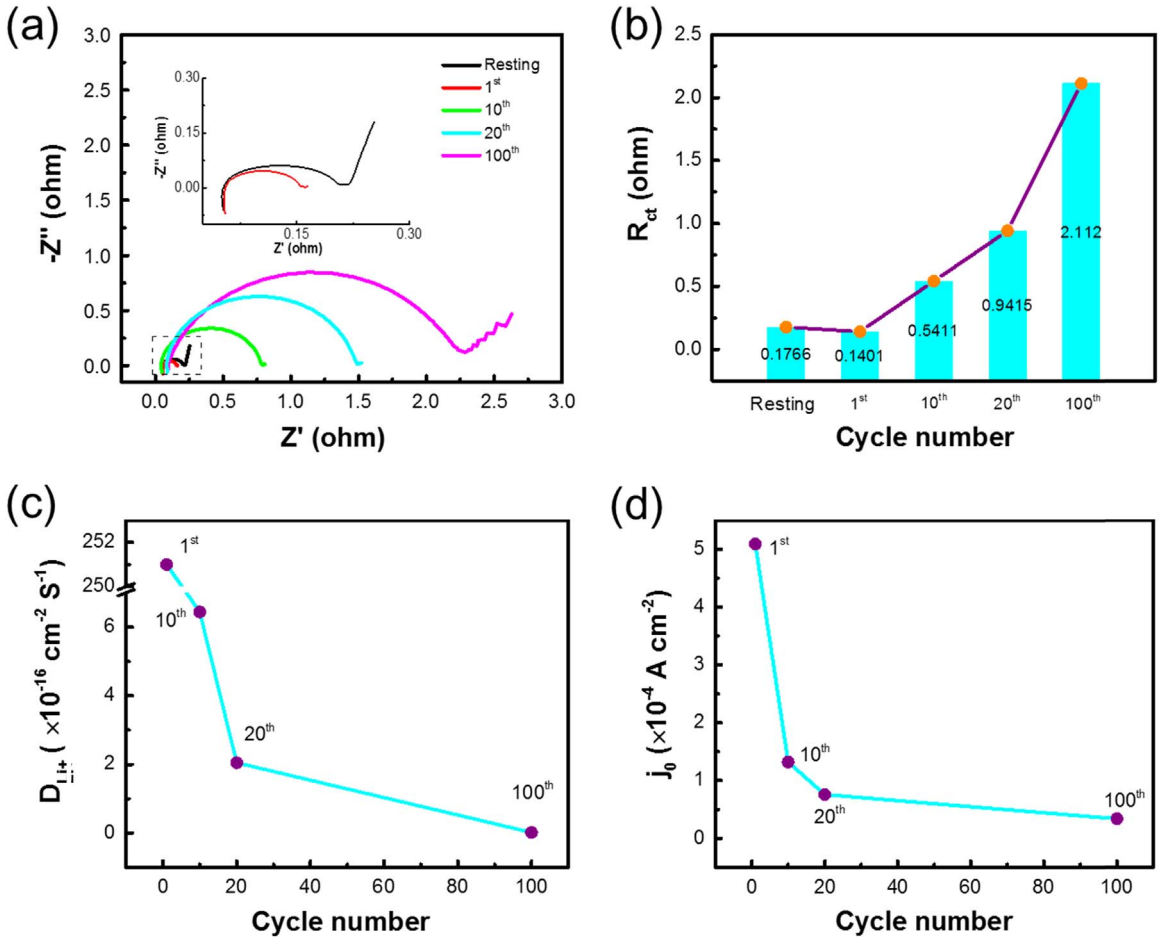

Fig. 5. Impedance characterization of Li-S pouch cells. (a) EIS of pouch cells. The inset figure is the locally enlarged image of the square area. (b) R_{ct} obtained from EIS curves. (c) Li ion diffusion coefficient (D_{Li+}) and (d) exchange current density (j_0) during cycles.

growth, but also recycle dead Li to be electronic contact with current collectors [36]. The conductive matrix can render Li metal anode a dendrite-free morphology, high electronic and ionic conductivities, and low volumetric change during Li plating/stripping. However, these anode matrices (including Li_7B_6 framework [56,57], glass fiber [58], graphene [36,37,59], 3D Cu current collector [60–62]) have not been applied into Li-S pouch cells. The compatibility between Li metal, electrolyte, and the anode matrix should been elaborately considered to achieve a long lifespan and high energy density Li-S pouch cells.

3. Conclusions

The gap between Li-S coin cell and pouch cell are probed and the failure mechanism for Li-S pouch cell was investigated. Compared with LiPS shuttle attributed to the failure of Li-S coin cell, the disabled Li metal anode contributes more to a failed pouch cell. Both dead Li and Li powdering caused by Li dendrite growth on the Li metal anode at large current resulted in the large polarization and finally terminated the lifespan of Li-S pouch cells. The Li ion diffusion coefficient and exchange current density of a pouch cell decreased from 2.51×10^{-14} to 1.50×10^{-18} cm^{-2} S^{-1} and 4.40×10^{-4} to 3.38×10^{-5} A cm^{-2} after testing for 100 cycle. Consequently, relatively to a neglected role in coin cells, Li metal anode tremendously affects long-term cycling performance of Li-S pouch cells. When the cycled Li anode was updated by a fresh Li metal, the renaissance cell with cycled cathode *vs* fresh anode indicated an improved discharge capacity from 314 to 1030 mA h g^{-1} at 0.1 C and remained stable in the following cycles (999 mA h g^{-1} at 15th cycle) with a high Coulombic efficiencies (78.13% at 15th cycle). To bridge the gap between Li-S coin and pouch cells, Li metal anode with stable SEI to prevent Li powdering and increase Li ion diffusion is urgently needed. More attentions should be concentrated on efficiently protecting Li metal anode to practical Li-S batteries.

4. Experimental section

4.1. Preparation of Li-S coin and pouch cell

The Li-S coin cell was fabricated according to a standard procedure in our previous publications [63,64]. The C/S composite cathodes were composed of sulfur (Alfa Aesar, $>99.9\%$) and carbon nanotubes according to a weight ratio of 7:3. Carboxymethyl cellulose (Alfa Aesar) and styrene butadiene rubber (Alfa Aesar) were mixed in a weight ratio of 1:1 in distilled water to be used as binder. The slurry was homogeneously stirred by mixing hollander at a rotation speed of 300 rpm. An intermittent roller was used to coat the slurry onto a 20 μm aluminum current collector. After drying the electrode at a vacuum atmosphere for 6.0 h at 60 °C, an areal sulfur loading of 4.43 mg cm^{-2} was obtained. Rectangles with a size of 30 mm × 50 mm were punched as the working cathodes for the Li-S pouch cells.

The Li anodes (China Energy Lithium Corporation, China) were also punched with the same shape as cathode. A layer-by-layer process has been used to alternate the cathodes and anodes with

Celgard 2400 polypropylene membranes acting as the separator in a Li-S pouch cell.

All the cathode and anode current collectors were controlled in parallel connection through an electrode lug terminal. 1.0 mol L^{-1} (M) lithium bis(trifluoromethanesulfonyl)imide (LiTFSI) as well as 2.0 wt% $LiNO_3$ additive dissolved in dimethyl ether (DME) and 1, 3-dioxolane (DOL) with a volume ratio of 1:1 was selected as electrolyte. Electrolyte with a ratio of 3 mL mg^{-1} sulfur was added into a pouch cell. Both the pouch cell and the coin cell are assembled in a glove box with O_2 and H_2O content below 1.0 ppm.

4.2. Electrochemical measurements and characterization

Both the coin cell and pouch cell were tested in a galvanostatic mode within a voltage range of 1.8–2.8 V in Land CT2001 multichannel battery tester. EIS of the cell was taken on Solartron 1470E electrochemical workstation in a frequency range of 1.0 MHz–0.1 Hz. All EIS measurements of the batteries were tested in the same voltage range. The morphology of anode was characterized by a field scanning electron microscope (SEM, JSM 7401F, JEOL Ltd., Tokyo, Japan) at 3.0 kV.

4.3. Methods to disassemble cells

After cycles, the coin and pouch cells were disassembled in a glove box with O_2 and H_2O content below 1.0 ppm to obtain the cycled cathode and anode samples for morphology characterization. The samples for SEM observation were prepared in the glovebox and transfered to a home-made sealed box to prevent the corrosion of air, especially water. The optical images of the electrodes were also obtained in the glovebox. To describe the large reaction activity of cycled Li induced by Li powdering in a cycled pouch cell, the cycled Li metal anode was taken out of glovebox and exposed to the air. However, it should be noted that due to its large reaction activity, the powdery Li has to be handled in dry atmosphere and must be put in a relatively open areas with special care.

Acknowledgments

This work was supported by National Key Research and Development Program (Nos. 2016YFA0202500 and 2016YFA0200102) and Natural Scientific Foundation of China (Nos. 21422604 and 21676160). We thank Rui Zhang, Chen-Zi Zhao, and Chao Guan for helpful discussion.

Appendix A. Supplementary material

Supplementary data associated with this article can be found in the online version at http://dx.doi.org/10.1016/j.ensm.2016.09.003.

References

[1] J.M. Tarascon, M. Armand, Nature 414 (2001) 359–367.
[2] R. Chen, R. Luo, Y. Huang, F. Wu, L. Li, Adv. Sci. (2016) 1600051.
[3] W. Lv, Z. Li, Y. Deng, Q.-H. Yang, F. Kang, Energy Storage Mater. 2 (2016) 107–138.
[4] X.-B. Cheng, R. Zhang, C.-Z. Zhao, F. Wei, J.-G. Zhang, Q. Zhang, Adv. Sci. 3 (2016) 1500213.
[5] R.G. Cao, W. Xu, D.P. Lv, J. Xiao, J.G. Zhang, Adv. Energy Mater. 5 (2015) 1402273.
[6] J. Qian, W.A. Henderson, W. Xu, P. Bhattacharya, M. Engelhard, O. Borodin, J. G. Zhang, Nat. Commun. 6 (2015) 6362.
[7] A. Manthiram, S.H. Chung, C. Zu, Adv. Mater. 27 (2015) 1980–2006.
[8] Y.X. Yin, S. Xin, Y.G. Guo, L.J. Wan, Angew. Chem. Int. Ed. 52 (2013) 13186–13200.
[9] M. Yu, R. Li, M. Wu, G. Shi, Energy Storage Mater. 1 (2015) 51–73.
[10] J.Q. Huang, Q. Zhang, F. Wei, Energy Storage Mater. 1 (2015) 127–145.
[11] J. Liang, Z.-H. Sun, F. Li, H.-M. Cheng, Energy Storage Mater. 2 (2016) 76–106.
[12] Z. Li, Y. Huang, L. Yuan, Z. Hao, Y. Huang, Carbon 92 (2015) 41–63.
[13] S. Risse, S. Angioletti-Uberti, J. Dzubiella, M. Ballauff, J. Power Sources 267 (2014) 648–654.
[14] C. Monroe, J. Newman, J. Electrochem. Soc. 152 (2005) A396–A404.
[15] C.-Z. Zhao, X.-B. Cheng, R. Zhang, H.-J. Peng, J.-Q. Huang, R. Ran, Z.-H. Huang, F. Wei, Q. Zhang, Energy Storage Mater. 3 (2016) 77–84.
[16] C. Lai, Z.Z. Wu, X.X. Gu, C. Wang, K. Xi, R.V. Kumar, S.Q. Zhang, ACS Appl. Mater. Interfaces 7 (2015) 23885–23892.
[17] H.-J. Peng, J.-Q. Huang, M.-Q. Zhao, Q. Zhang, X.-B. Cheng, X.-Y. Liu, W.-Z. Qian, F. Wei, Adv. Funct. Mater. 24 (2014) 2772–2781.
[18] C. Zhang, Q.H. Yang, Sci. China Mater. 58 (2015) 349–354.
[19] R. Fang, S. Zhao, P. Hou, M. Cheng, S. Wang, H.-M. Cheng, C. Liu, F. Li, Adv. Mater. 28 (2016) 3374–3382.
[20] S.Z. Niu, W. Lv, C. Zhang, F.F. Li, L.K. Tang, Y.B. He, B.H. Li, Q.H. Yang, F.Y. Kang, J. Mater. Chem. A 3 (2015) 20218–20224.
[21] H.-J. Peng, T.-Z. Hou, Q. Zhang, J.-Q. Huang, X.-B. Cheng, M.-Q. Guo, Z. Yuan, L.-Y. He, F. Wei, Adv. Mater. Interfaces 1 (2014) 1400227.
[22] X.Y. Tao, J.G. Wang, C. Liu, H.T. Wang, H.B. Yao, G.Y. Zheng, Z.W. Seh, Q.X. Cai, W.Y. Li, G.M. Zhou, C.X. Zu, Y. Cui, Nat. Commun. 7 (2016) 11203.
[23] S. Rehman, S.J. Guo, Y.L. Hou, Adv. Mater. 28 (2016) 3167–3172.
[24] J. Zhang, H. Hu, Z. Li, X.W. Lou, Angew. Chem. Int. Ed. 55 (2016) 3982–3986.
[25] Y. Wei, Y. Tao, Z. Kong, L. Liu, J. Wang, W. Qiao, L. Ling, D. Long, Energy Storage Mater. 5 (2016) 171–179.
[26] H. Yao, K. Yan, W. Li, G. Zheng, D. Kong, Z.W. Seh, V.K. Narasimhan, Z. Liang, Y. Cui, Energy Environ. Sci. 7 (2014) 3381–3390.
[27] J.Q. Huang, Q. Zhang, H.J. Peng, X.Y. Liu, W.Z. Qian, F. Wei, Energy Environ. Sci. 7 (2014) 347–353.
[28] G.M. Zhou, L. Li, D.W. Wang, X.Y. Shan, S.F. Pei, F. Li, H.M. Cheng, Adv. Mater. 27 (2015) 641–647.
[29] H.J. Peng, D.W. Wang, J.Q. Huang, X.B. Cheng, Z. Yuan, F. Wei, Q. Zhang, Adv. Sci. 3 (2016) 1500268.
[30] J.R. Nair, F. Bella, N. Angulakshmi, A.M. Stephan, C. Gerbaldi, Energy Storage Mater. 3 (2016) 69–76.
[31] C. Masquelier, Nat. Mater. 10 (2011) 649–650.
[32] Z. Chen, P.-C. Hsu, J. Lopez, Y. Li, J.W.F. To, N. Liu, C. Wang, Sean C. Andrews, J. Liu, Y. Cui, Z. Bao, Nat. Energy 1 (2016) 15009.
[33] F. Ding, W. Xu, G.L. Graff, J. Zhang, M.L. Sushko, X. Chen, Y. Shao, M. H. Engelhard, Z. Nie, J. Xiao, X. Liu, P.V. Sushko, J. Liu, J.G. Zhang, J. Am. Chem. Soc. 135 (2013) 4450–4456.
[34] N.W. Li, Y.X. Yin, C.P. Yang, Y.G. Guo, Adv. Mater. 28 (2016) 1853–1858.
[35] C. Yan, X.-B. Cheng, C.-Z. Zhao, J.-Q. Huang, S.-T. Yang, Q. Zhang, J. Power Sources 327 (2016) 212–220.
[36] X.-B. Cheng, H.-J. Peng, J.-Q. Huang, R. Zhang, C.-Z. Zhao, Q. Zhang, ACS Nano 9 (2015) 6373–6382.
[37] R. Zhang, X.B. Cheng, C.Z. Zhao, H.J. Peng, J.L. Shi, J.Q. Huang, J.F. Wang, F. Wei, Q. Zhang, Adv. Mater. 28 (2016) 2155–2162.
[38] W. Li, H. Yao, K. Yan, G. Zheng, Z. Liang, Y.M. Chiang, Y. Cui, Nat. Commun. 6 (2015) 7436.
[39] W. Zhou, B. Guo, H. Gao, J.B. Goodenough, Adv. Energy Mater. 6 (2016) 1502059.
[40] L. Qie, A. Manthiram, ACS Energy Lett. 1 (2016) 46–51.
[41] Z. Wei Seh, W. Li, J.J. Cha, G. Zheng, Y. Yang, M.T. McDowell, P.-C. Hsu, Y. Cui, Nat. Commun. 4 (2013) 1331.
[42] M.K. Song, Y. Zhang, E.J. Cairns, Nano Lett. 13 (2013) 5891–5899.
[43] C. Luo, Y. Zhu, O. Borodin, T. Gao, X. Fan, Y. Xu, K. Xu, C. Wang, Adv. Funct. Mater. 26 (2016) 745–752.
[44] L. Gireaud, S. Grugeon, S. Laruelle, B. Yrieix, J.M. Tarascon, Electrochem. Commun. 8 (2006) 1639–1649.
[45] L. Qie, C.X. Zu, A. Manthiram, Adv. Energy Mater. 6 (2016) 1502459.
[46] S. Liu, G.R. Li, X.P. Gao, ACS Appl. Mater. Interfaces 8 (2016) 7783–7789.
[47] G.Q. Ma, Z.Y. Wen, M.F. Wu, C. Shen, Q.S. Wang, J. Jin, X.W. Wu, Chem. Commun. 50 (2014) 14209–14212.
[48] D. Aurbach, E. Pollak, R. Elazari, G. Salitra, C.S. Kelley, J. Affinito, J. Electrochem. Soc. 156 (2009) A694–A702.
[49] X.B. Cheng, H.J. Peng, J.Q. Huang, R. Zhang, C.Z. Zhao, Q. Zhang, ACS Nano 9 (2015) 6373–6382.
[50] H. Liu, C. Li, H.P. Zhang, L.J. Fu, Y.P. Wu, H.Q. Wu, J. Power Sources 159 (2006) 717–720.
[51] Q. Liu, C. Du, B. Shen, P. Zuo, X. Cheng, Y. Ma, G. Yin, Y. Gao, RSC Adv. 6 (2016) 88683–88700.
[52] C. Zu, N. Azimi, Z. Zhang, A. Manthiram, J. Mater. Chem. A 3 (2015) 14864–14870.
[53] Y.Y. Lu, Z.Y. Tu, L.A. Archer, Nat. Mater. 13 (2014) 961–969.
[54] H. Xiang, P. Shi, P. Bhattacharya, X. Chen, D. Mei, M.E. Bowden, J. Zheng, J.-G. Zhang, W. Xu, J. Power Sources 318 (2016) 170–177.
[55] L. Suo, Y.-S. Hu, H. Li, M. Armand, L. Chen, Nat. Commun. 4 (2013) 1481.
[56] X.-B. Cheng, H.-J. Peng, J.-Q. Huang, F. Wei, Q. Zhang, Small 10 (2014) 4257–4263.
[57] X. Zhang, W. Wang, A. Wang, Y. Huang, K. Yuan, Z. Yu, J. Qiu, Y. Yang, J. Mater. Chem. A 2 (2014) 11660–11665.
[58] X.-B. Cheng, T.-Z. Hou, R. Zhang, H.-J. Peng, C.-Z. Zhao, J.-Q. Huang, Q. Zhang, Adv. Mater. 28 (2016) 2888–2895.

[59] D. Lin, Y. Liu, Z. Liang, H.-W. Lee, J. Sun, H. Wang, K. Yan, J. Xie, Y. Cui, Nat. Nanotechnol. 11 (2016) 626–632.
[60] L.-L. Lu, J. Ge, J.-N. Yang, S.-M. Chen, H.-B. Yao, F. Zhou, S.-H. Yu, Nano Lett. 16 (2016) 4431–4437.
[61] C.-P. Yang, Y.-X. Yin, S.-F. Zhang, N.-W. Li, Y.-G. Guo, Nat. Commun. 6 (2015) 8058.
[62] Q. Yun, Y.-B. He, W. Lv, Y. Zhao, B. Li, F. Kang, Q.-H. Yang, Adv. Mater. 28 (2016) 6932–6939.
[63] M.-Q. Zhao, Q. Zhang, J.-Q. Huang, G.-L. Tian, J.-Q. Nie, H.-J. Peng, F. Wei, Nat. Commun. 5 (2014) 3410.
[64] C. Tang, Q. Zhang, M.Q. Zhao, J.Q. Huang, X.B. Cheng, G.L. Tian, H.J. Peng, F. Wei, Adv. Mater. 26 (2014) 6100–6105.